Int. J. Solids Structures, 1977, Vol. 13, pp. 503–514. Pergamon Press. Printed in Great Britain

ELASTO-PLASTIC RESPONSE OF A MULTI-LAYERED SPHERICAL VESSEL TO INTERNAL BLAST LOADING

W. L. Ko,† H. G. Pennick and W. E. Baker
Southwest Research Institute, San Antonio, TX 78284, U.S.A.

(*Received* 2 *July* 1976)

Abstract—Dynamic response of a multi-layered spherical vessel subjected to intermittent internal blast loading is analysed. The vessel is composed of N concentric unsupported spherical shells of identical material and of the same thickness, separated by evacuated gaps of equal thickness. The wall material is assumed to be elasto-plastic obeying the bilinear stress-strain law. Taking into account of the wave interactions induced by inter-laminar impacts, response of the vessel system was calculated up to five cycles of vibration and the results are presented for several gap sizes.

INTRODUCTION

Gastight structures (or vessels) have wide engineering applications. Examples of such structures include: (1) Blast chamber, within which the effects of explosives or propellants can be studied under controlled atmospheric conditions. (2) Safety chambers, for proof testing of small pressure vessels. (3) Nuclear-reactor containment structures designed to contain the effects of accidental runaway of the reactors which they house.

Because these structures must be able to withstand static as well as transient internal pressures without bursting, they are usually constructed in the forms of spherical shells or cylindrical shells with spherical end caps.

In designing such structures, knowledge of their response to the worst loading conditions is needed. The most simple geometry for analytical study is the spherical shells. Mono-layered spherical shells subjected to internal blast loading have been studied extensively, for example, by Baker *et al.*[1–3].

For better performance of such a spherical shell structure, the shell may be composed of several laminae with or without interlaminar gaps.

This paper concerns the analysis of such multi-layered elasto-plastic spherical shells subjected to spherically symmetric intermittent internal blast loading.

By considering elasto-plastic wave interactions due to mutual impacts of wall laminae, the response of the structure was calculated up to five cycles of vibration and the results are presented for several interlaminar gap sizes.

DESCRIPTION OF PROBLEM

The multi-layered spherical vessel structure is composed of N number of concentric unsupported thin spherical shells (or laminae) of identical material each with the same thickness h. The wall laminae are separated by evacuated gaps of equal thickness g (see Fig. 1). Material of the laminae is assumed to be elasto-plastic obeying the bilinear stress-strain law.

The innermost lamina (or layer) is subjected to spherically symmetric intermittent internal blast loading $p(t)$ where t is time. The problem is to calculate the response of the vessel system due to $p(t)$, accounting for the wave interactions induced by inter-laminar inpacts.

ANALYSIS

When the multi-layered spherical vessel is subjected to internal blast loading of intensity $p(t)$, layer 1 will be excited and move alone radially outward with a certain velocity (single layer motion). When layer 1 strikes on layer 2, wave interaction between the two layers will take place. During this contact period the two layers will move jointly (joint motion). At the end of wave interaction, the two layers will separate and move independently (single layer motion). Layer 2 will then strike on layer 3 and induce similar interaction motions. This type of interactions will propagate outwardly to a certain layer [determined by the intensity of $p(t)$] and then propagate inwardly again, and so forth.

†Now at NASA Dryden Flight Research Center, Edwards, CA 93523, U.S.A.

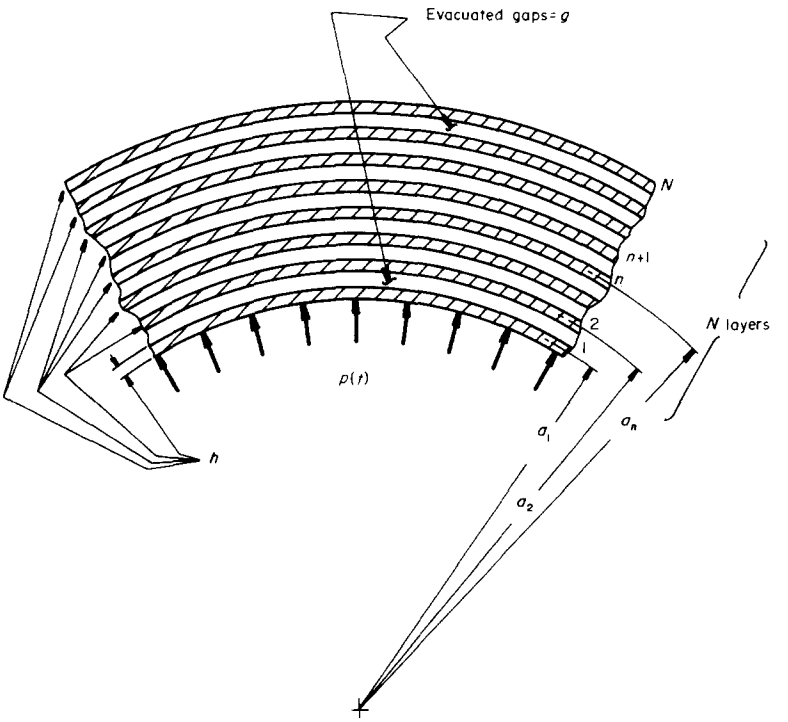

Fig. 1. Section of multi-layered spherical vessel subjected to internal blast loading.

(a) *Single layer motion*

When layer n ($n = 1,2,3,\ldots N$) is deformed elastically and is moving by itself, its radial displacement $u_n(t)$ can be determined by solving the following equation of motion[1]

$$\ddot{u}_n(t) + \omega_n^2 u_n(t) = \frac{p(t)}{\rho h}\delta_{n1} \tag{1}$$

together with certain initial conditions [e.g. for layer 1, $\dot{u}_1(0) = u_1(0) = 0$ at $t = 0$]. In eqn (1) ρ is the density of the wall laminae, $[\ddot{\ }] \equiv (d^2/dt^2)[\ ]$, δ_{n1} is the Kronecker delta, and ω_n is the circular frequency of layer n defined as[1]

$$\omega_n^2 = \frac{2E}{\rho a_n^2(1-\nu)} \tag{2}$$

where a_n is the radius of layer n, E is the Young's modulus, and ν is the Poisson's ratio.

For the larger spacing between layers, the shell can deform plastically and the equation of motion for the plastic loading response is given by[1]

$$\ddot{u}_n(t) + \frac{2S}{\rho a_n^2}u_n(t) = \frac{p(t)}{\rho h}\delta_{n1} - \frac{2(\sigma_Y - S\epsilon_Y)}{\rho a_n}; \qquad \dot{u}_n(t) > 0 \tag{3}$$

where S is the slope of the plastic portion of the bilinear biaxial stress-strain curve (identical in θ and ϕ direction due to spherical symmetry), σ_Y† and $\epsilon_Y[= \sigma_Y(1-\nu)/E]$ are respectively the biaxial yield stress and yield strain when the radial stress is absent, (see Fig. 2). Equation (3) holds until the positive velocity $\dot{u}_n(t)$ reaches zero.

For unloading from the plastic regime (point B in Fig. 2) and reloading along line BC up to point B, the motion of the shell is then governed by the elastic equation of motion:

$$\ddot{u}_n(t) + \omega_n^2 u_n(t) = \frac{p(t)}{\rho h}\delta_{n1} + \omega_n^2 \bar{u}_n \tag{4}$$

where $\bar{u}_n(\equiv a_n\bar{\epsilon})$ is the permanent displacement associated with the residual strain $\bar{\epsilon}$ (see Fig. 2).

†For the present problem where two of the circumferential normal stress components $\sigma_{\theta\theta}$ and $\sigma_{\phi\phi}$ are equal and the third is zero (except layer 1), the biaxial yield stress σ_Y is equal to the uniaxial yield stress according to von Mises yield criterion.

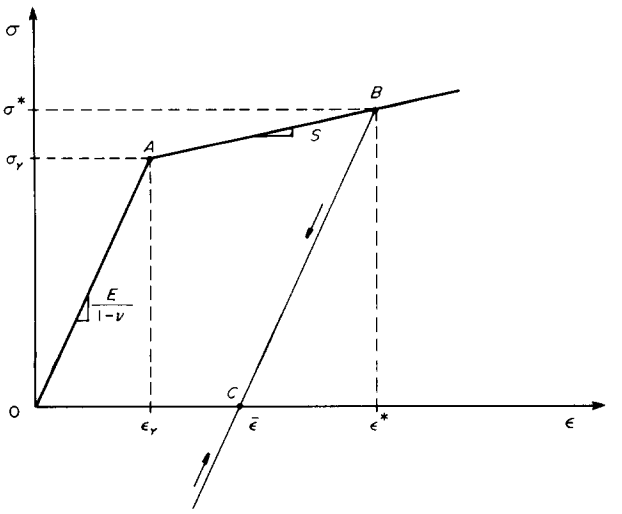

Fig. 2. Bi-linear stress-strain curve for circumferential direction θ or ϕ. $\sigma \equiv \sigma_{\theta\theta} = \sigma_{\phi\phi}$, $\epsilon \equiv \epsilon_{\theta\theta} = \epsilon_{\phi\phi}$ due to spherical symmetry.

For reloading beyond point B, eqn (3) is again applicable but, $\{\sigma_Y, \epsilon_Y\}$ in the equation must be replaced by $\{\sigma^*, \epsilon^*\}$, the stress and strain corresponding to point B.

(b) *Wave interactions*

When the vessel is subjected to the blast loading $p(t)$, two types of waves [stress or shock waves depending on the intensity of $p(t)$] can be generated in the wall laminae: (i) waves induced by the inter-laminar impacts, (ii) waves arising from the transmission of $p(t)$ into the wall laminae.

If the intensities of the waves (or stress levels) induced by the interlaminar impacts are more severe than those induced by $p(t)$, and if the rise time of each pulse of $p(t)$ is very much longer (say, two or three orders of magnitude longer) than the wave transit time across the thickness of the layer as in the present problem, the waves generated by $p(t)$ may be neglected, and only the first type of wave interactions will be considered.

If at $t = t_n$, layer n, which is moving at a velocity $\dot{u}_n(t_n)$, strikes layer $n+1$ which is moving at a slower velocity $\dot{u}_{n+1}(t_n)$,† two compressive waves of intensity $|\sigma_{rr}| = \sigma_{rr}^*$ (see Fig. 3) will be sent out and travel in opposite directions from the interface.

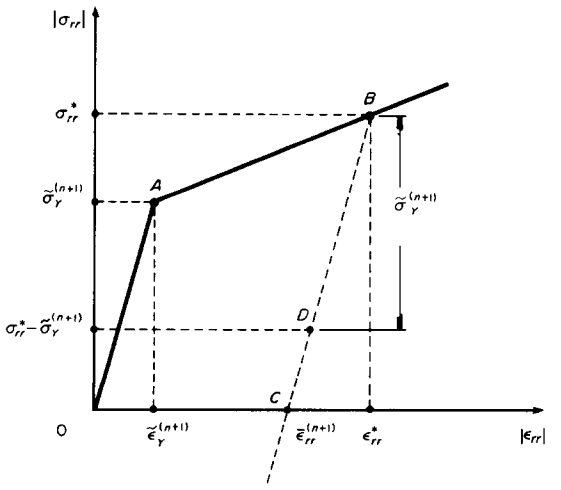

Fig. 3. Bilinear compressive stress-strain curve in radial direction (for layer $n+1$).

†For the first impact $\dot{u}_{n+1}(t_n) = 0$.

If the impact is elastic (i.e. $|\sigma_{rr}^* - \sigma_{\theta\theta}| < \sigma_Y$), each wave will propagate at the elastic wave velocity C given by

$$C = \sqrt{\left(\frac{\lambda + 2\mu}{\rho}\right)} = \sqrt{\left(\frac{E}{\rho}\right)} \sqrt{\left(\frac{1-\nu}{(1+\nu)(1-2\nu)}\right)} \tag{5}$$

where λ and μ are the Lamé constants.

If the impact induced deformation is plastic (i.e. $|\sigma_{rr}^* - \sigma_{\theta\theta}| > \sigma_Y$), the compressive wave of intensity σ_{rr}^* in each layer will travel at the spherical plastic wave velocity U given by[4, 5]

$$U = \sqrt{\left(\frac{E}{\rho}\right)} \sqrt{\left(\frac{1+(1-2\nu)\beta}{(1-2\nu)[3-(1-2\nu)\beta]}\right)} \xrightarrow[\beta \to 1]{} C \tag{6}$$

where $\beta E (0 < \beta \leq 1)$ is the slope of plastic portion of the bilinear uniaxial stress–strain curve. These plastic waves in layer n and $n+1$ will be preceded respectively by faster moving elastic precursors of intensities $\tilde{\sigma}_Y^{(n)} (\equiv |\sigma_Y - \sigma_{\theta\theta}^{(n)}|)$ and $\tilde{\sigma}_Y^{(n+1)} (\equiv |\sigma_Y - \sigma_{\theta\theta}^{(n+1)}|)$ propagating at velocity C. As will be seen immediately below, $\tilde{\sigma}_Y^{(n)}$ in general is not equal to $\tilde{\sigma}_Y^{(n+1)}$. It is seen from eqns (5) and (6) that when $\beta = 1$ (i.e. purely elastic) we have $U = C$ as is expected.

Figure 4 shows the stress states in layers n and $n+1$ before and after impact, appearing in the stress plane passing through σ_{rr} and $\sqrt{(2)}\sigma_{\theta\theta}$ axes and axis of the von Mises yield surface. Immediately before impact, layer n, which has been deformed is under equi-biaxial tension† in circumferential direction as indicated by point P. At the instant of impact ($t = t_n$), the impact induced radial compressive stress $-\sigma_{rr}^*$ will cause $\sigma_{\theta\theta}$ (or $\sigma_{\phi\phi}$) behind the wave front to decrease from point P down to point P' (or $\sqrt{(2)}\sigma_{\theta\theta}^{(n)}$) due to circumferential constraint. Thus, the stress state in layer n will be shifted from point P to point P''. The radial compressive yield stress in layer n will then be $-\tilde{\sigma}_Y^{(n)}$. Similarly, in layer $n+1$, the stress state Q before the impact will be shifted to point Q'' after the impact. For this particular case, the circumferential stress in layer $n+1$ will be purely compressive [i.e., $\sigma_{\theta\theta} = -\sigma_{\theta\theta}^{(n+1)}$ (point Q')]. The radial compressive yield stress for this layer will then be $-\tilde{\sigma}_Y^{(n+1)}$ whose magnitude is much larger than that of $-\tilde{\sigma}_Y^{(n)}$.

Figure 5 shows histories of stress, strain and particle velocity distributions in layer $n+1$ and stress history in layer n after it has hit layer $n+1$ from the left hand side at the impact time $t = t_n$. Due to similarity, histories of strain and particle velocity for layer n are not shown. We will

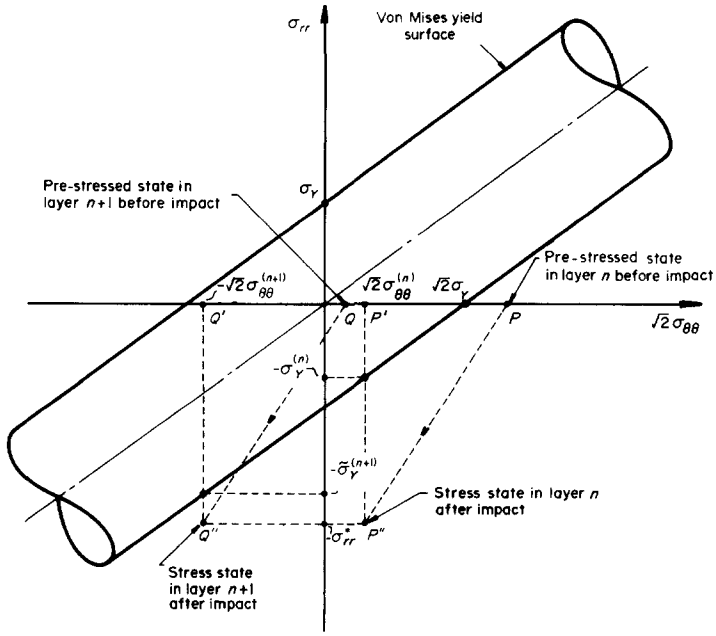

Fig. 4. Stress states in layers n and $n+1$ before and after impact.

†Outgoing impact is discussed here.

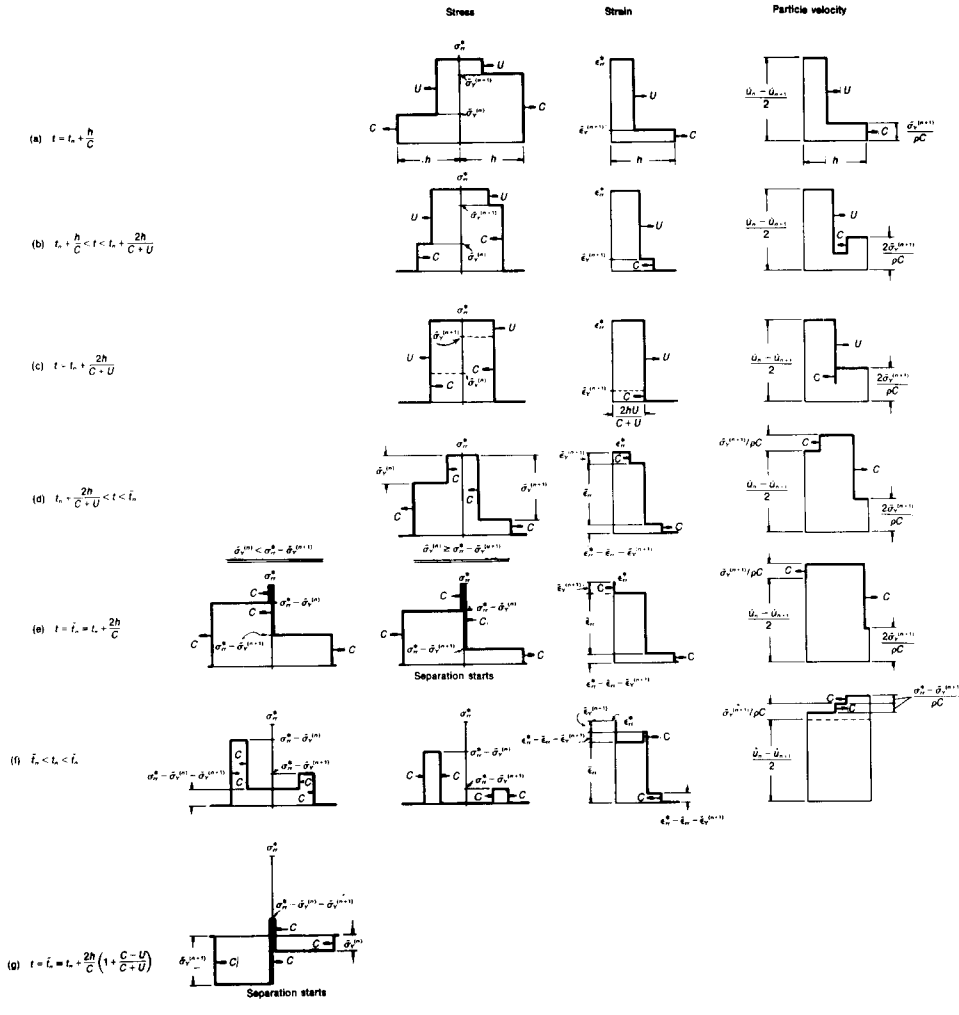

Fig. 5. Histories of stress, strain and particle velocity distributions in layer $n+1$ after impact with layer n at left.

discuss mainly the wave interactions in layer $n+1$. At stage (a) ($t = t_n + h/C$), the elastic precursor has just reached the free surface of the layer on the right hand side. The particle velocity (relative to the undisturbed region of the layer) in the region behind the elastic precursor and ahead of the plastic wave front is $\tilde{\sigma}_Y^{(n+1)}/\rho C$ [6] and the particle velocity in the region behind the plastic wave front is $(1/2)[\dot{u}_n(t_n) - \dot{u}_{n+1}(t_n)]$ [7]. After the elastic precursor is reflected at the free surface, it becomes an unloading wave of intensity $\tilde{\sigma}_Y^{(n+1)}$, behind which the material becomes stress free and the original particle velocity increases by an amount $\tilde{\sigma}_Y^{(n+1)}/\rho C$ [Stage (b)]. At $t = t_n + 2h/(C+U)$ [Stage (c)], the reflected elastic unloading wave and the plastic loading wave will meet. From this point on [Stage (d)], the plastic wave will be unloaded by an amount $\tilde{\sigma}_Y^{(n+1)}$ along the unloading curve BC down to point D in Fig. 3, and turn into an elastic wave with reduced intensity $\sigma_{rr}^* - \tilde{\sigma}_Y^{(n+1)}$, moving at velocity C. Stage (e) shows the instant ($t = \bar{t}_n \equiv t_n + 2h/C$) the reflected unloading elastic precursor has just reached the interface. The material in the region bounded by the interface and a surface at a distance $2hU/(C+U)$ from the interface, will now be permanently deformed with residual strain $\bar{\epsilon}_{rr}^{(n+1)}$ (see Fig. 3). If $\tilde{\sigma}_Y^{(n)} \geq \sigma_{rr}^* - \tilde{\sigma}_Y^{(n+1)}$, i.e., the intensity $\tilde{\sigma}_Y^{(n)}$ of the unloading wave from layer n is just equal to or greater than the intensity $\sigma_{rr}^* - \tilde{\sigma}_Y^{(n+1)}$ of the reduced compressive wave in layer $n+1$, the interfacial compressive stress $\sigma_{rr}^* - \tilde{\sigma}_Y^{(n+1)}$ will be reduced to zero at the instant ($t = \bar{t}_n$) the unloading wave from layer n reaches the interface. Thus, the two layers will separate at this moment and move with different velocities. After layer separation [Stage (f)], the "residual" waves will continue to travel and interact in each layer until dissipated.

If, on the other hand, $\tilde{\sigma}_Y^{(n)} < \sigma_{rr}^* - \tilde{\sigma}_Y^{(n+1)}$, then the unloading wave from layer n is not intense

enough to nullify the reduced compressive wave in layer $n+1$ at the instant $t = \bar{t}_n$. Thus, the two layers will continue to be in contact after $t = \bar{t}_n$ [Stage (f)]. This contact will last until the reduced compressive wave is reflected at the free surface as an unloading wave of intensity $\sigma_{rr}^* - \tilde{\sigma}_Y^{(n+1)}$ and travel back and reaches the interface at $t = \tilde{t}_n \equiv t_n + (2h/C)[1 + (C-U)/(C+U)]$ [Stage (g)]. After layer separation, like the previous case, "residual" waves will remain in each layer for a while before dying-out.

For the material properties and geometry used in the present problem, the wave transit time (across the layer thickness) is in the order of 10^{-6} sec., and the time interval between the two successive impacts is in the order of 10^{-3} sec. This means that the "residual" waves will travel back and forth across the layer thickness several thousands times until next impact. Hence, we will assume that the "residual" waves will die out or attenuate sufficiently before the next impact and, therefore, their influence on the subsequent impacts will be ignored.

From the conservation of momentum across the plastic wave front, the intensity of initial plastic wave σ_{rr}^* may be expressed as[8]

$$\sigma_{rr} - \tilde{\sigma}_Y^{(i)} = \rho\left[U - \frac{\tilde{\sigma}_Y^{(i)}}{\rho C}\right]\left[\frac{1}{2}\{\dot{u}_n(t_n) - \dot{u}_{n+1}(t_n)\} - \frac{\tilde{\sigma}_Y^{(i)}}{\rho C}\right]; \quad (i = n, n+1) \tag{7}$$

where $\tilde{\sigma}_Y^{(i)}/\rho C$ is the particle velocity in the region lying between the plastic wave front and the elastic precursor. Since the particle velocities are much less than the wave velocities, eqn (7) may be written approximately as follows, neglecting terms containing product of particle velocities:

$$\sigma_{rr}^* \approx \frac{\rho U}{2}[\dot{u}_n(t_n) - \dot{u}_{n+1}(t_n)] + \tilde{\sigma}_Y^{(i)}\left[1 - \frac{U}{C}\right]. \tag{8}$$

In the light of eqn (8) and Fig. 5(e), layer n will take off at time $\bar{t}_n$ (for $\tilde{\sigma}_Y^{(n)} \geq \sigma_{rr}^* - \tilde{\sigma}_Y^{(n+1)}$) with absolute velocity given by†

$$\dot{u}_n(\bar{t}_n) = \dot{u}_n(t_n) - \frac{1}{2}[\dot{u}_n(t_n) - \dot{u}_{n+1}(t_n)] - \frac{\tilde{\sigma}_Y^{(n)}}{\rho C} \tag{9}$$

$$= \frac{\dot{u}_n(t_n)}{2}\left[1 - \frac{U}{C}\frac{\tilde{\sigma}_Y^{(n)}}{\sigma_{rr}^*}\right] + \frac{\dot{u}_{n+1}(t_n)}{2}\left[1 + \frac{U}{C}\frac{\tilde{\sigma}_Y^{(n)}}{\sigma_{rr}^*}\right] - \frac{\tilde{\sigma}_Y^{(n)}}{\rho C}\left[1 - \frac{U}{C}\right]\frac{\tilde{\sigma}_Y^{(n)}}{\sigma_{rr}^*} \tag{10}$$

and layer $n+1$ will take off at the same instant $\bar{t}_n$ (for $\tilde{\sigma}_Y^{(n)} \geq \sigma_{rr}^* - \tilde{\sigma}_Y^{(n+1)}$) with absolute velocity given by

$$\dot{u}_{n+1}(\bar{t}_n) = \dot{u}_{n+1}(t_n) + \frac{1}{2}[\dot{u}_n(t_n) - \dot{u}_{n+1}(t_n)] + \frac{\tilde{\sigma}_Y^{(n+1)}}{\rho C} \tag{11}$$

$$= \frac{\dot{u}_n(t_n)}{2}\left[1 + \frac{U}{C}\frac{\tilde{\sigma}_Y^{(n+1)}}{\sigma_{rr}^*}\right] + \frac{\dot{u}_{n+1}(t_n)}{2}\left[1 - \frac{U}{C}\frac{\tilde{\sigma}_Y^{(n+1)}}{\sigma_{rr}^*}\right] + \frac{\tilde{\sigma}_Y^{(n+1)}}{\rho C}\left[1 - \frac{U}{C}\right]\frac{\tilde{\sigma}_Y^{(n+1)}}{\sigma_{rr}^*}. \tag{12}$$

For the case $\tilde{\sigma}_Y^{(n)} < \sigma_{rr}^* - \tilde{\sigma}_Y^{(n+1)}$, layer n will take off at $t = \tilde{t}_n$ [see Fig. 5(g)] with absolute velocity:

$$\dot{u}_n(\tilde{t}_n) = \dot{u}_n(t_n) - \frac{1}{2}[\dot{u}_n(t_n) - \dot{u}_{n+1}(t_n)] - \frac{\tilde{\sigma}_Y^{(n)}}{\rho C} - \frac{\sigma_{rr}^* - \tilde{\sigma}_Y^{(n)}}{\rho C} + \frac{\tilde{\sigma}_Y^{(n+1)}}{\rho C} \tag{13}$$

$$= \frac{\dot{u}_n(t_n)}{2}\left[1 - \frac{U}{C}\right] + \frac{\dot{u}_{n+1}(t_n)}{2}\left[1 + \frac{U}{C}\right] + \frac{\tilde{\sigma}_Y^{(n+1)}}{\rho C}\frac{U}{C}[1 - \delta_{UC}] \tag{14}$$

and layer $n+1$ will take off at $t = \tilde{t}_n$ with the absolute velocity:

$$\dot{u}_{n+1}(\tilde{t}_n) = \dot{u}_{n+1}(t_n) + \frac{1}{2}[\dot{u}_n(t_n) - \dot{u}_{n+1}(t_n)] + \frac{\tilde{\sigma}_Y^{(n+1)}}{\rho C} + \frac{\sigma_{rr}^* - \tilde{\sigma}_Y^{(n+1)}}{\rho C} - \frac{\tilde{\sigma}_Y^{(n)}}{\rho C} \tag{15}$$

$$= \frac{\dot{u}_n(t_n)}{2}\left[1 + \frac{U}{C}\right] + \frac{\dot{u}_{n+1}(t_n)}{2}\left[1 - \frac{U}{C}\right] - \frac{\tilde{\sigma}_Y^{(n)}}{\rho C}\frac{U}{C}[1 - \delta_{UC}]. \tag{16}$$

†Neglecting temporarily the join motion effect which is analyzed subsequently.

In eqns (14) and (16), which were obtained by the aid of eqn (8), δ_{UC} is the Kronecker delta (i.e. $\delta_{UC} = 1$ if $U = C$, $\delta_{UC} = 0$, if $U \neq C$).

(c) *Joint motion during impact*

During the impact contact period ($t_n \leq t \leq \bar{t}_n$), or ($t_n \leq t \leq \tilde{t}_n$), layers n and $n+1$ will move jointly, and the motion can be described by the following joint equations of motion if the two layers deform elastically:

$$\ddot{u}_{n+(n+1)}(t) + \frac{1}{2}[\omega_n^2 + \omega_{n+1}^2]u_{n+(n+1)}(t) = \frac{p(t)}{2\rho h}\delta_{n1} - \frac{\omega_n^2 u_n(t_n)}{2} - \frac{\omega_{n+1}^2 u_{n+1}(t_n)}{2}; \quad (t_n \leq t \leq \bar{t}_n) \text{ or } (t_n \leq t \leq \tilde{t}_n) \tag{17}$$

$$u_{n+(n+1)}(t_n) = 0, \quad \dot{u}_{n+(n+1)}(t_n) = \frac{1}{m_n + m_{n+1}}[m_n\dot{u}_n(t_n) + m_{n+1}\dot{u}_{n+1}(t_n)]; \quad (t = t_n) \tag{18}$$

where $u_{n+(n+1)}(t)$ is the joint displacement measured from the configuration at t_n and $m_i (i = n, n+1)$ is the mass of layer i.

Equation (17) is obtained by writing separate equations of motion for the two layers and then combining them into one equation by eliminating the inter-laminar pressure term. The last two terms on the right hand side of the equation are the prestress terms.

If layer n undergoes plastic deformation and layer $n+1$ is elastic, the joint equations of motion will be

Loading:

$$\ddot{u}_{n+(n+1)}(t) + \frac{1}{2}\left[\frac{2S}{\rho a_n^2} + \omega_{n+1}^2\right]u_{n+(n+1)}(t) = \frac{p(t)}{2\rho h}\delta_{n1} - \frac{\sigma_Y^{(n)} - S\epsilon_Y^{(n)}}{\rho a_n} - \frac{Su_n(t_n)}{\rho a_n^2} - \frac{\omega_{n+1}^2 u_{n+1}(t_n)}{2}; \quad (t_n \leq t \leq \bar{t}_n) \text{ or } (t_n \leq t \leq \tilde{t}_n). \tag{19}$$

where $\sigma_Y^{(n)}$ and $\epsilon_Y^{(n)}$ are the circumferential yield stress and strain in layer n after impact ($\sigma_Y^{(n)} = \sigma_{\theta\theta}^{(n)}$ in Fig. 4).

Unloading:

$$\ddot{u}_{n+(n+1)}(t) + \frac{1}{2}[\omega_n^2 + \omega_{n+1}^2]u_{n+(n+1)}(t) = \frac{p(t)}{2\rho h}\delta_{n1} - \frac{\omega_n^2}{2}[u_n(t_n) - \bar{u}_n] - \frac{\omega_{n+1}^2}{2}u_{n+1}(t_n); \quad (t_n \leq t \leq \bar{t}_n) \text{ or } (t_n \leq t \leq \tilde{t}_n) \tag{20}$$

where $\bar{u}_n$ is the residual displacement of layer n.

If both of the layers deform plastically, then the equations of motion will be of the forms:

Loading:

$$\ddot{u}_{n+(n+1)}(t) + \frac{S}{\rho}\left[\frac{1}{a_n^2} + \frac{1}{a_{n+1}^2}\right]u_{n+(n+1)}(t) = \frac{p(t)}{2\rho h}\delta_{n1} - \frac{1}{\rho}\left[\frac{\sigma_Y^{(n)} - S\epsilon_Y^{(n)}}{a_n} + \frac{\sigma_Y^{(n+1)} - S\epsilon_Y^{(n+1)}}{a_{n+1}}\right] - \frac{S}{\rho}\left[\frac{u_n(t_n)}{a_n^2} + \frac{u_{n+1}(t_n)}{a_{n+1}^2}\right] \quad (t_n \leq t \leq \bar{t}_n) \text{ or } (t_n \leq t \leq \tilde{t}_n) \tag{21}$$

where $\sigma_Y^{(n+1)}$ and $\epsilon_Y^{(n+1)}$ are the circumferential yield stress and strain in layer $n+1$ after impact ($\sigma_Y^{(n+1)} = -\sigma_{\theta\theta}^{(n+1)}$ in Fig. 4)

Unloading:

$$\ddot{u}_{n+(n+1)}(t) + \frac{1}{2}[\omega_n^2 + \omega_{n+1}^2]u_{n+(n+1)}(t) = \frac{p(t)}{2\rho h}\delta_{n1} - \frac{1}{2}\omega_n^2[u_n(t_n) - \bar{u}_n] - \frac{1}{2}\omega_{n+1}^2[u_{n+1}(t_n) - \bar{u}_{n+1}] \quad (t_n \leq t \leq \bar{t}_n) \text{ or } (t_n \leq t \leq \tilde{t}_n) \tag{22}$$

where $\bar{u}_{n+1}$ is the residual displacement of layer $n+1$.

At the end of the contact, ($t = \bar{t}_n$ or $t = \tilde{t}_n$) both layers will gain velocity by an amount

$$\Delta\dot{u}_{n+(n+1)} = \begin{cases} \dot{u}_{n+(n+1)}(\bar{t}_n) - \dot{u}_{n+(n+1)}(t_n), & \tilde{\sigma}_Y^{(n)} \geq \sigma_{rr}^* - \tilde{\sigma}_Y^{(n+1)} \\ \dot{u}_{n+(n+1)}(\tilde{t}_n) - \dot{u}_{n+(n+1)}(t_n), & \tilde{\sigma}_Y^{(n)} < \sigma_{rr}^* - \tilde{\sigma}_Y^{(n+1)}. \end{cases} \tag{23}$$

This velocity change, which is the most severe for $n = 1$ due to the action of $p(t)$, must then be added to eqns (10) and (12) or eqns (14) and (16).

After separation, single layer equations of motion will again be applicable.

The above solution process can now march on for the subsequent impacts.

NUMERICAL SOLUTIONS

For the vessel response calculations, the loading function $p(t)$ shown in Fig. 6 was used. The broken curve is a rectified pressure-time history for certain blast loading. The solid curve is the adjusted "worst case" loading condition for which all the pulses except the first one are shifted slightly with respect to the first one so that the peak-to-peak duration is 2τ where τ is the period of vibration for Layer 1 based on the vessel properties given below. This "worst case" loading condition was used in the response calculations.

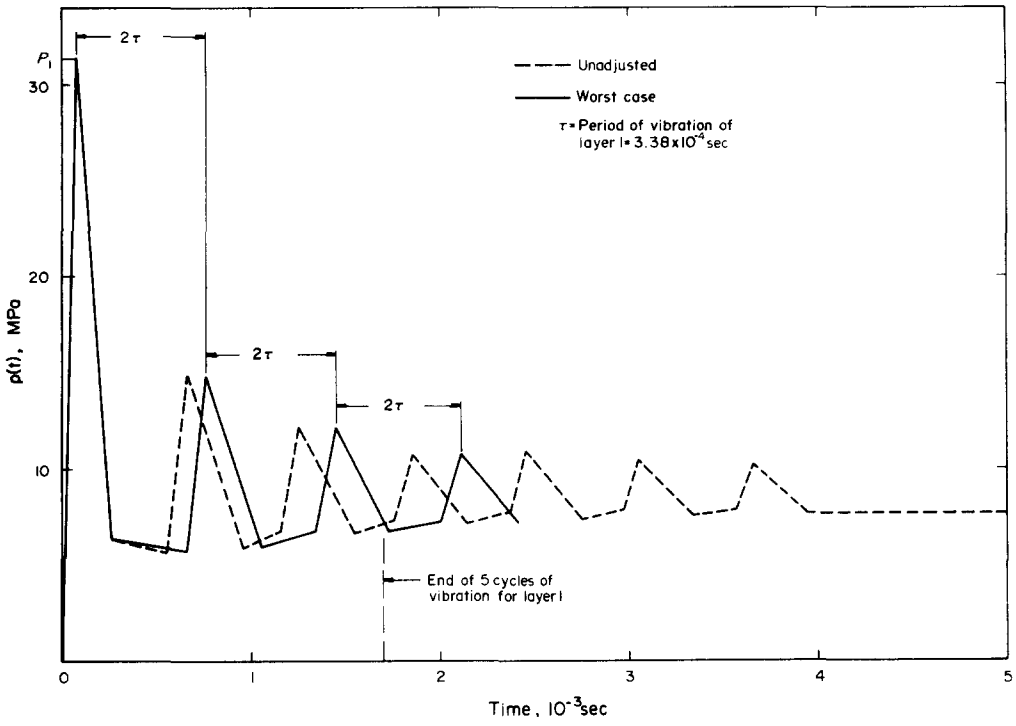

Fig. 6. Pressure-time histories of blast loadings.

Due to the complexity of the loading function $p(t)$, the shell equations of motion were solved numerically by using finite difference method.

For the response calculations, the shell material was assumed to be A 537 steel having the following properties:

Young's modulus	$E = 0.2$ TPa
Plastic modulus (uniaxial)	$S_{uni} = 1.205$ GPa
Yield strength (uniaxial or equi-biaxial)	$\sigma_Y = 0.34$ GPa
Ultimate strength (uniaxial)	$\sigma_u = 0.48$ GPa
Poisson's ratio	$\nu = 0.29$
Density	$\rho = 7.8$ Mg/m^3

and the vessel has the following dimensions:

Inside radius	$a_0 = 0.457$ m	Interlaminar gaps	$g = 1$ mm, 6.35 mm
Lamina thickness	$h = 3.18$ mm	Number of layers	$N = 8$

RESULTS

Using the input parameters given earlier, the responses of the vessel were calculated up to five cycles of vibration. The results are presented in Figs. 7–10. In each figure the yield displacement $u_n^Y (n = 1, \ldots 8)$ for each layer is shown.

Figure 7 shows the "worst case" response of the vessel system having inter-laminar gap of $g = 1$ mm when the inter-laminar impact is elasto-plastic. It is seen that only the inner five layers are disturbed and the rest remains intact. All the disturbed layers deform plastically. Most of the impacts take place between the adjacent layers (2-layer impacts). For a few instances another layer will come into impact with the two layers which are still in the process of wave interaction (3-layer impacts, shown by arrows in the figure). Since the present computer program will not assess the 3-layer impacts, we slightly adjusted the 2-layer impact duration so that the third layer will come into impact with one of the two layers after they separate. Errors introduced by this adjustment are insignificant because the time duration for the two-layer wave interaction (i.e. between contact and separation) is in the order of 10^{-6} sec, which is pictorically invisible in the figures where the time scale is 10^{-3} sec. For refinement of the vessel response calculations, the 3-layer impact wave interactions must be analysed.

For the purpose of comparison, a result for elastic inter-laminar impacts is shown in Fig. 8 for the $g = 1$ mm case. This calculation was made by simply setting $U = C$ for the impact waves. The shell motion is still governed by the same set of elastoplastic equations of motion used for the previous case. Notice that all the eight layers are disturbed and deform plastically. One 3-layer impact (between layers 3.4 and 5) occurs at $t = 0.808$ m sec (indicated by an arrow in the figure). The rest of the inter-laminar impacts are two layer impacts.

Figure 9 shows the "worst case" response of the vessel walls with maximum gap $g = 6.35$ mm when the inter-laminar impact is elasto-plastic. Notice that the inner three layers undergo large plastic deformations and the fourth layer, small plastic deformation. During the early stage ($0 < t < 0.95$ m sec) of vessel response, the inner three layers move very closely with frequent "clapping" (weak inter-laminar impacts). After $t = 0.95$ m sec the inter-laminar gaps grow and the occurrence of inter-laminar impacts becomes less frequent. Note that the 3-layer impacts (between layers 1, 2 and 3) occur only twice, the rest are 2-layer impacts.

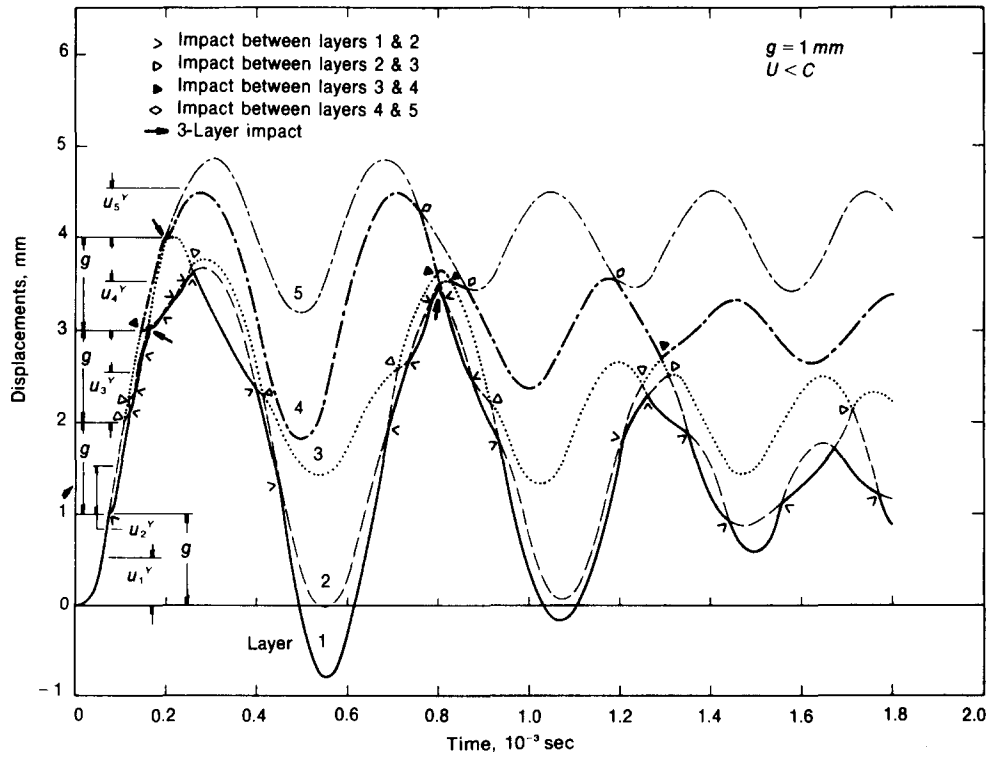

Fig. 7. Displacement-time histories of spherical vessel wall laminae ($g = 1$ mm, elasto-plastic inter-laminar impacts).

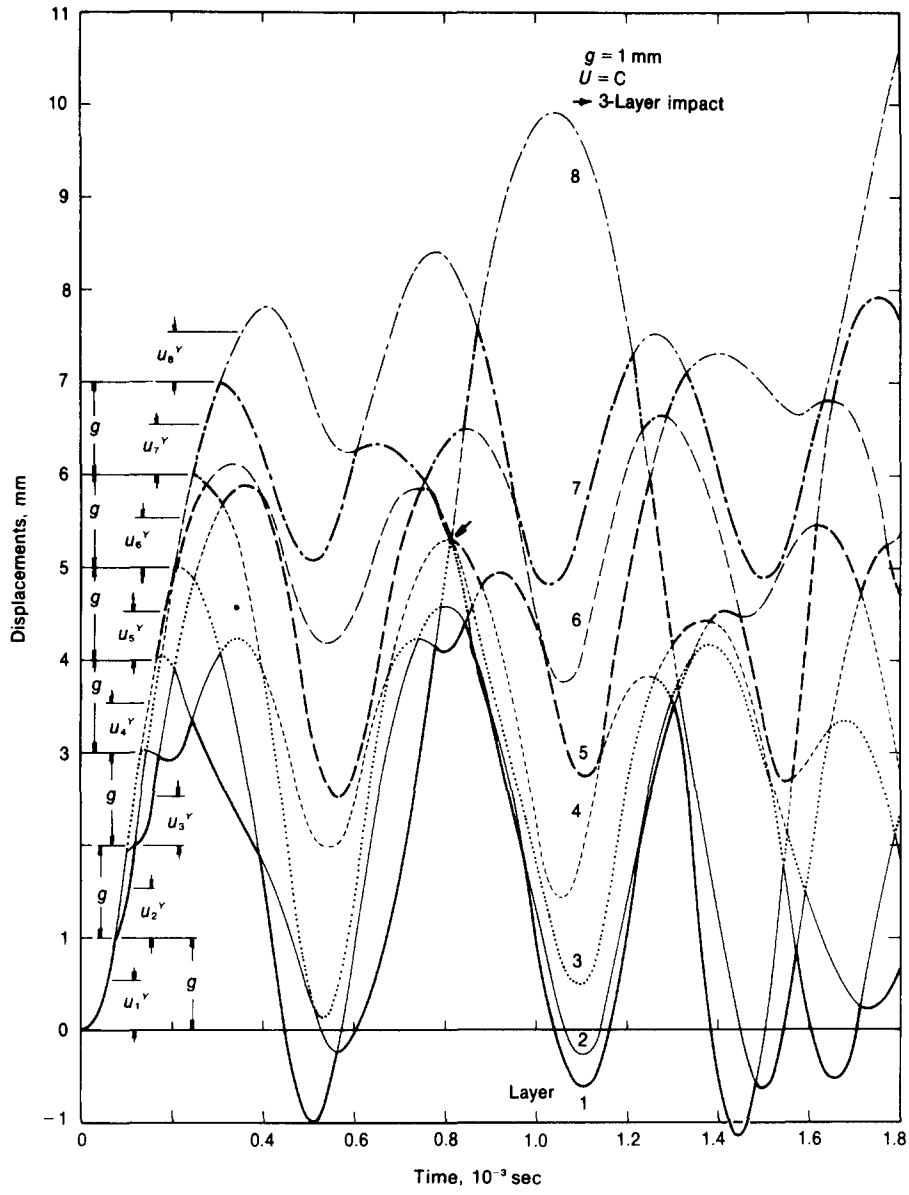

Fig. 8. Displacement-time histories of spherical vessel wall laminae (g = 1 mm, elastic interlaminar impacts).

Figure 10 shows the maximum gap ($g = 6.35$ mm) case for elastic inter-laminar impacts ($U = C$). In contrast to elasto-plastic impacts (Fig. 9), the blast load is felt up to the seventh layer. All the disturbed layers except the seventh one experience large plastic deformations. Notice that all the inter-laminar impacts are two layer impacts which take place less frequently as compared with Fig. 9.

SUMMARY

We have analysed the motion of multi-layered elasto-plastic spherical vessels with inter-laminar gaps, generated by the internal blast loading, and have presented numerical examples of the vessel responses.

Under the given loading condition, all the disturbed layers undergo plastic deformations. In most cases, the inner layers suffer the most severe plastic deformations.

If the time span is extended, it is likely that the chances for multiple inter-laminar impacts can arise. Therefore, for future study the elasto-plastic wave interactions arising from the multiple-layer impacts must be analysed.

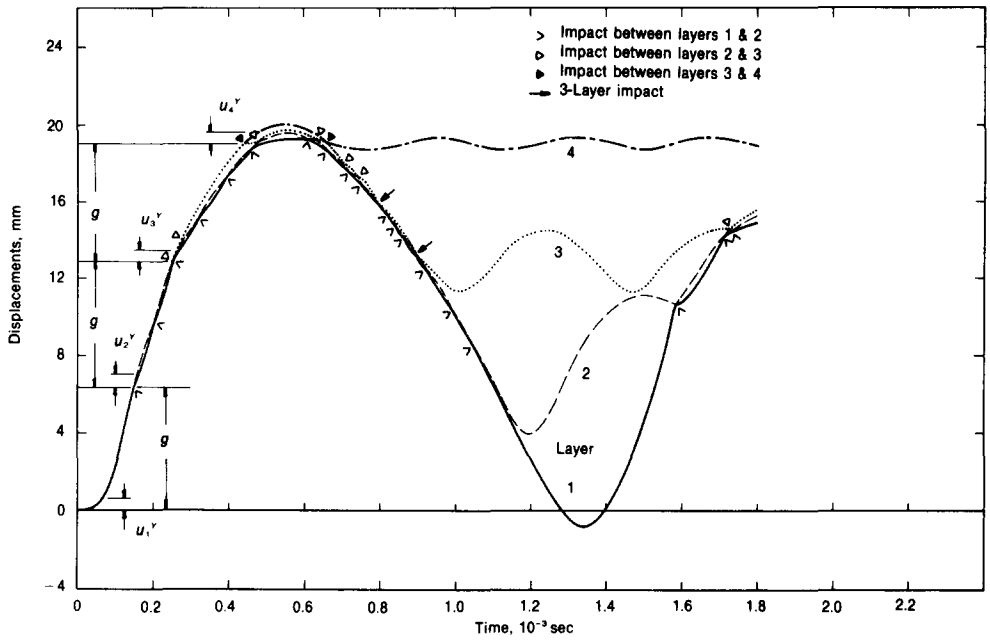

Fig. 9. Displacement-time histories of spherical vessel wall laminae ($g = 6.35$ mm, elasto-plastic inter-laminar impacts).

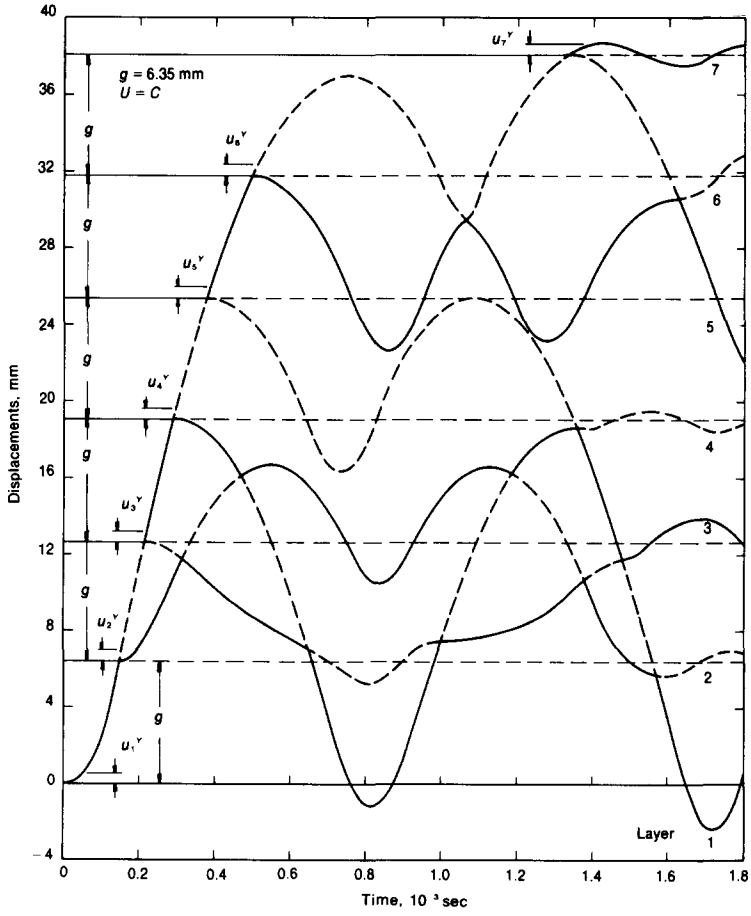

Fig. 10. Displacement-time histories of spherical vessel wall laminae ($g = 6.35$ mm, elastic inter-laminar impacts).

Acknowledgement—The research reported in this paper was sponsored by the University of California Los Alamo Scientific Laboratory, under Contract P. O. LP5-92905-3.

REFERENCES

1. W. E. Baker, The elastic-plastic response of thin spherical shells to internal blast loading. *J. Appl. Mech.*, **27**, Series E, No. 1, 139–144, (March 1960).
2. W. E. Baker, W. C. L. Hu and T. R. Jackson, Elastic response of thin spherical shells to axisymmetric blast loading. *J. Appl. Mech.*, **33**, Series E, No. 4, 800–806 (December 1966).
3. W. E. Baker and F. J. Allen, The response of elastic spherical shells to spherically symmetric internal blast loading. *Proc. Third Int. Congr. Appl. Mech. ASME*, pp. 79–87, (1958).
4. M. G. Srinivasan and T. C. T. Ting, Initiation of spherical elastic-plastic boundaries due to loading at a spherical cavity. *J. Mech. Phys. Solids* **22**, 415–435 (1974).
5. M. G. Srinivasan, Reflection and transmission of elastic-plastic spherical waves at a spherical interface. *ASME Paper No.* 75 WA/APM-23 (1975).
6. H. Kolsky, *Stress Waves in Solids*. Dover, New York (1963).
7. S. Timoshenko and J. N. Goodier, *Theory of Elasticity*, 2nd Edn. McGraw-Hill, New York (1951).
8. O. E. Jones, Metal response under explosive loading. *Behavior and Utilization of Explosives in Engineering Design, 12th Annual Symp.* (March 1972).